

## Removal of phosphate from aqueous solutions by adsorption onto $\text{Ca}(\text{OH})_2$ treated natural clinoptilolite

Dimitris Mitrogiannis<sup>\*a</sup>, Maria Psychoyou<sup>a</sup>, Ioannis Baziotis<sup>a</sup>, Vassilis J. Inglezakis<sup>b</sup>,  
Nikolaos Koukouzas<sup>c</sup>, Nikolaos Tsoukalas<sup>c</sup>, Dimitrios Palles<sup>d</sup>, Efstratios Kamitsos<sup>d</sup>,  
Georgios Oikonomou<sup>e</sup>, Giorgos Markou<sup>a</sup>

<sup>a</sup> Department of Natural Resources Management and Agricultural Engineering,  
Agricultural University of Athens, 75 Iera Odos, 11855 Athens, Greece

<sup>b</sup> School of Engineering, **Chemical Engineering Department, Environmental Science &  
Technology Group (ESTg)**, Nazarbayev University, 53, Kabanbay batyr ave., 010000  
Astana, Republic of Kazakhstan

<sup>c</sup> Centre for Research and Technology Hellas (CERTH), Chemical Process and Energy  
Resources Institute (CPERI), 52 Egialias str., 15125 Maroussi, Athens, Greece

<sup>d</sup> Theoretical and Physical Chemistry Institute, National Hellenic Research Foundation,  
48 Vassileos Constantinou Avenue, Athens 11635, Greece

<sup>e</sup> Institute of Geology and Mineral Exploration, Olympic Village Acharnae, Athens,  
Greece, P.C. 13677

\* Corresponding author: E-mail: [mitrogdimi@gmail.com](mailto:mitrogdimi@gmail.com)

Telephone: +30 6974876236

## Abstract

Phosphorus (P) recovery from wastewater is of great interest especially when the loaded adsorbent can be used in the agriculture as slow-release fertilizer. The application depends on environmental concerns related to the chemical modification of the adsorbent and the release of toxic compounds from the loaded material to the soil or the water during adsorption. The present work focused on the phosphate ( $\text{PO}_4\text{-P}$ ) removal from aqueous solutions under low P concentrations (0.5-10 mg/L) by using  $\text{Ca}(\text{OH})_2$ -pretreated natural zeolite (CaT-Z). As activation agent,  $\text{Ca}(\text{OH})_2$  presents benefits in terms of pretreatment costs and environmental impact of the applied adsorbent. The pretreatment of natural zeolite (clinoptilolite) with 0.25 mol/L  $\text{Ca}(\text{OH})_2$  led to an increase of P removal from 1.7 to 97.6% at initial P concentration of 10 mg/L, pH 7 and 298 K. A significant reduction of the soluble reactive P was achieved with low residual concentrations of 81-238  $\mu\text{g P/L}$  at 298 K rendering CaT-Z a promising sorbent for tertiary wastewater treatment. At 200 mg P/L, the adsorption capacity was 7.57 mg P/g CaT-Z. The P removal efficiency was pH-independent suggesting a beneficial use of CaT-Z under acidic and alkaline conditions. Adsorption was found to be an endothermic and slow process reaching equilibrium after 120 h, whereas the half of the  $\text{PO}_4\text{-P}$  was adsorbed in the first 8 h. The applied kinetic models showed that both film and intraparticle diffusion contributed to phosphate removal. Phosphate sorption decreased in the presence of the anionic surfactant SDS,  $\text{Fe}^{2+}$ ,  $\text{HCO}_3^-$ , acetate and citrate anion. The predominant mechanisms of ligand exchange and Ca-P surface precipitation were confirmed by the IR-ATR and SEM-EDS analyses, respectively.

**Keywords:** *zeolite; phosphate adsorption; ligand exchange; surface precipitation; diffusion; eutrophication*

## **1. Introduction**

Phosphorus (P) is an essential macroelement for plant and algae growth, but its excessive presence as phosphate ( $\text{PO}_4^{3-}$ ) in aquatic ecosystems can lead to deterioration of water quality due to eutrophication [1]. High amounts of phosphate can cause algal blooms and depletion of dissolved oxygen in the water bodies with negative impacts on the aquatic organisms [2]. Human activities such as animal manure and fertilizer application in soil or discharge of industrial, domestic and agricultural wastewater are responsible for the enrichment of surface waters with phosphate loadings [1, 3, 4].

Various physical, chemical and biological methods have been **proposed** for phosphate removal from water or wastewater such as anion exchange, sorption, chemical precipitation, membrane nanofiltration, reverse osmosis, electrodialysis and biological removal through constructed wetland, activated sludge and microalgal systems [4, 5]. In practice, the most widely used methods are biological removal and chemical precipitation. Nevertheless, they also present limitations such as undesired waste sludge production or dependence on water temperature and organic load regarding the biological removal, whereas chemical precipitation requires high input of chemical reagents (Ca, Mg, Al and Fe salts). **On the other hand, adsorption by using minerals** is considered as an efficient, simple and low-cost method for  $\text{PO}_4\text{-P}$  removal even at low phosphate concentrations [4, 6, 7]. However, the surface modification of **natural minerals is needed to change** their

surface charge from negative to positive and to enable them to adsorb phosphate anions [4].

Numerous modified mineral adsorbents have been tested for phosphate removal at low (<10 mg/L), medium (10-100 mg/L) and high (> 100 mg/L) initial P concentrations [8-12]. However, there is a particular interest in adsorbents which can efficiently treat solutions of low initial P concentrations and exhibit low residual concentrations in the order of ppb ( $\mu\text{g/L}$ ) in the effluents [4, 11]. These concentrations are required from the legislations of European Union and other countries concerning municipal wastewater treatment [4, 13]. An important parameter in sorption process is the adsorbent particle size, which is related to adsorption capacity, kinetics and separation of the adsorbent from the liquid phase. Sorbing materials of larger particle size exhibit sufficient hydraulic conductivity and could be employed more effective in fixed-bed columns or in constructed wetland systems where the adsorbent is used as support medium for plants in order to minimize the clogging and enhance the contact between wastewater and substrate [4, 14, 15]. Additionally, phosphate adsorbents can be used as P-inactivation agents in lake sediments operating as active barrier layer at the sediment-water interface for the reduction of the sediments internal P loading [1, 8].

Despite the good phosphate adsorption capacity of natural minerals modified with polyvalent metals such as  $\text{Zr}^{4+}$ ,  $\text{La}^{3+}$ ,  $\text{Al}^{3+}$  or  $\text{Fe}^{3+}$ , there is the risk of toxic effects on aquatic species and deterioration of water quality by the release of these metals, especially  $\text{Al}^{3+}$  and  $\text{Fe}^{3+}$ , under redox or acidic conditions [8, 12, 16]. Moreover, the chemical reagents of rare earth elements (REEs), such as  $\text{La}^{3+}$  used for the commercial modified bentonite

(Phoslock®), or zirconium are much more expensive than those of  $\text{Ca}^{2+}$ ,  $\text{Mg}^{2+}$ ,  $\text{Fe}^{3+}$  and  $\text{Al}^{3+}$  [17, 18]. It should be noted that the European Commission has labelled REEs and magnesium as critical raw materials in terms of increasing prices, high import dependency and access difficulty due to possible political tensions or shortage [17]. Therefore, the development of more cost-effective, **local available** and environmental friendly pretreatment methods for adsorbent modification is desired, especially when the nutrient-loaded sorbents can be applied in the agriculture as fertilizers with no restrictions related to the modification reagents. The release of the exchangeable or impregnated cations **such as**  $\text{K}^+$ ,  $\text{Na}^+$ ,  $\text{Ca}^{2+}$  and  $\text{Mg}^{2+}$  by natural or modified zeolites during adsorption processes has **no environmental impacts** since these cations are considered as non-toxic [19].

Previous studies have shown the enhanced phosphate sorption onto calcium-rich minerals such as thermally-treated palygorskite [8, 9], calcined sepiolite [20],  $\text{CaCO}_3$ -montmorillonite [21], CaO-modified bentonite [22] and  $\text{Ca}(\text{OH})_2$  treated bentonite [23]. A benefit of phosphate loaded adsorbents can be their use as slow-release fertilizers in agriculture [24, 25] or microalgae cultivation [26]. According to the literature [24, 27], P bound to Ca phases of the soil is more plant available than P bound to Al and Fe oxides of clay particles, and P recovery from wastewater as calcium phosphate presented agronomic effectiveness as a fertilizer material. It is important to **develop** adsorbents containing Ca able to bind P and release it at a slow rate corresponding to the P requirements of the growing plants in order to achieve higher yields and less surface runoff of P. In contrast, easily soluble P fertilizers can become less plant available during

the growth period due to strong P sorption on soil clay particles [24]. Calcium hydroxide and oxide present advantages in terms of environmental impact and chemical **cost** of **adsorbent** pretreatment since lime is the cheapest source of Ca (0.006 US\$/mol) [28] and  $\text{Ca(OH)}_2$  is cheaper (0.08 US\$/kg) than Mg salts [29] commonly used in **minerals** modification [30]. **Furthermore, the** calcination of various **minerals** at high temperatures, i.e. > 973 K [8, 9, 20], in order to enhance their phosphate adsorption capacity, **requires energy and thus increases the pretreatment cost**. The pretreatment of adsorbents with  $\text{Ca(OH)}_2$  has been poorly investigated and the derived **adsorbents have not yet** been examined **thoroughly at** low initial P concentrations aiming at low levels ( $\mu\text{g/L}$ ) **of residual P**.

The present study focuses on the phosphate removal from aqueous solutions containing low P concentrations (0.5-10 mg/L) by using for the first time **a**  $\text{Ca(OH)}_2$  pretreated zeolite (CaT-Z). These P concentrations are typical for the effluents of municipal wastewater treatment obtained by activated sludge or small trickling filter plants [6]. The zeolite (clinoptilolite) exhibits ion sieving properties and higher cation-exchange capacity, thus it has a different adsorption behaviour than the  $\text{Ca(OH)}_2$  treated bentonite which was tested in a previous study in solutions with higher P concentrations (25-300 mg/L) [23]. In this study, the optimization of the natural zeolite (NZ) modification was examined by minimizing the amount of  $\text{Ca(OH)}_2$  used in the pretreatment in order to achieve the highest P removal efficiency. The effect of solution pH, contact time, initial P concentration, temperature and coexisting **substances** on the P removal by CaT-Z was investigated in batch **process**. A sequential desorption procedure was applied to **study** the

adsorption mechanisms of phosphate onto CaT-Z. A range of spectroscopic techniques (XRD, SEM-EDS, IR-ATR) were also used to characterize the sorbing material and to further determine the exact adsorption mechanisms at low and high P concentrations, 10 and 100 mg/L, respectively.

## **2. Materials and methods**

### **2.1. Adsorbent pretreatment and chemicals**

The natural zeolite (NZ) used as adsorbent in this study was commercially purchased (Thessaloniki, North Greece). The zeolite was sieved to particle sizes in the range of 1.19-2 mm. The material was washed several times firstly with tap and then with deionized water (DI), and dried overnight in an oven at 343 K. The chemical pretreatment of NZ was performed by adding the latter to solutions with five different concentrations of  $\text{Ca}(\text{OH})_2$  (0.01, 0.1, 0.25, 0.5 and 1 mol/L) at a zeolite/liquid ratio of 100 g/L. The mixture was shaken for 24 h at 298 K and 200 rpm. After that, the pretreated zeolite (CaT-Z) was washed several times with DI to remove excess  $\text{Ca}(\text{OH})_2$ , dried overnight at 343 K and stored in a sealed plastic vial until its use in adsorption tests. All reagents used in this study were of analytical grade (Merck, Sigma-Aldrich, Ferak), except humic acid (technical grade, Sigma-Aldrich).

### **2.2. Characterization of adsorbent**

#### **2.2.1 Scanning Electron Microscopy (SEM)**

The texture, mineral neo-formation and in-situ chemistry of the untreated NZ, CaT-Z and P-loaded CaT-Z was studied using SEM on a JEOL 6380 LV Scanning Electron Microscope equipped with Energy Dispersive System (EDS) INCAx-Sight 7388 at the Institute of Geology and Mineral Exploration (IGME), Athens (Greece). Images were captured from platinum-coated broken grains and polished thin sections at an accelerating voltage of 15-20 keV, a 20 nA beam current and 1-2  $\mu\text{m}$  beam diameter. For minerals, a 20 nA beam current and 20 s counting time on peak position were used. Natural minerals were used as standards as follows: corundum (Al), jadeite (Na), albite (Si), wollastonite (Ca), periclase (Mg), pyrite (Fe), orthoclase (K), rutile (Ti) and GaP (P).

### **2.2.2. X-Ray Diffraction (XRD)**

The powder XRD method was applied to identify the mineral phases in the untreated NZ, CaT-Z and P-loaded CaT-Z. The XRD patterns were obtained using a SIEMENS Diffractometer D-5000, X-ray source of Cu  $K\alpha$  ( $\lambda=1.54184 \text{ \AA}$ ) and Ni filter monochromator at the Centre of Research and Technology Hellas (Ptolemais, Greece). The conditions of the experiments were: diffraction angles  $2\theta$  from 3-70°, step size and rate 0.02°/sec, voltage of 35 kV and current of 25 mA. The XRD patterns were evaluated using the software DIFFRAC.EVA v4.1.

### **2.2.3. Infrared-Attenuated Total Reflectance (IR-ATR)**

The IR-ATR spectra were collected with a Bruker-Equinox 55 spectrometer at the National Hellenic Research Foundation, Theoretical and Physical Chemistry Institute



(Athens, Greece) in order to evaluate the mechanism of the phosphate uptake from the treated CaT-Z. The ATR accessory is equipped with a single-reflection diamond crystal and a spring-loaded mechanical press for compacting solid samples. Each IR-ATR spectrum represents an average of 100 scans in the 525–5000  $\text{cm}^{-1}$  spectral range with 4  $\text{cm}^{-1}$  resolution, with its intensity axis being corrected to account for the frequency dependent penetration depth of the IR radiation into the sample.

#### 2.2.4. Surface point of zero charge

To determine the point of zero charge ( $\text{pH}_{\text{pzc}}$ ) of the untreated NZ and CaT-Z surface, 200 mg adsorbent was added in 20 ml solution of 0.1 M NaCl at initial pH values of 5, 7, 9 and 10, adjusted with HCl or NaOH. The samples were stirred for 48 h at 298 K, and the final solution pH was recorded with a pH-meter (Metrohm 827). The difference between the initial and final pH ( $\text{pH}_i - \text{pH}_f$ ) was defined as  $\Delta\text{pH}$  and plotted against initial pH [23]. At point of zero charge  $\Delta\text{pH}$  equals to zero.

### 2.3. Adsorption experiments

All adsorption experiments were carried out in batch system at adsorbent dosage of 10 g/L by adding 200 mg CaT-Z and 20 mL phosphate solution into a 30 mL bottle of high-density polyethylene (HDPE). The solutions were agitated at 200 rpm with a horizontal shaker which was placed in a temperature controlled chamber. Phosphate stock solution of 200 mg P/L was prepared by dissolving the appropriate amount of  $\text{KH}_2\text{PO}_4$  in DI. The residual P concentration in the supernatant was measured without sample centrifugation

because the adsorbent material remained on the bottle bottom during the process. Phosphate concentration and adsorption capacity (see Eq. 1 and 2) were expressed as mg P/L and mg P/g, respectively, where 1 mg P/L = 3.066 mg PO<sub>4</sub><sup>3-</sup>/L [7]. The P concentration was measured by the ascorbic acid colorimetric method [31] using a UV-vis spectrophotometer at 880 nm (Hach-Lange 2800), whereas the equilibrium concentration of K<sup>+</sup> in the solution after adsorption at 100 mg P/L and 298 K was measured by flame photometer (BWB XP, UK). All experiments were performed in triplicate and their average values are given.

The effect of various Ca(OH)<sub>2</sub> treatments (0.01-1 M) of NZ on phosphate removal was investigated in solutions with two different initial P concentrations (10 and 100 mg/L) at pH 7, 298 K and for contact time of 120 h. The zeolite pretreated with 0.25 M Ca(OH)<sub>2</sub> was selected for further experiments.

The kinetics of phosphate sorption on CaT-Z were studied at initial P concentration of 10 and 100 mg/L. Kinetic tests were performed in 100 mL solution at pH 7 and 298 K using sealed plastic flasks of 200 mL. For the first 24 h of the experiment, samples (50 µL) were collected at 0.25, 0.5, 1, 1.5, 2, 3, 4, 8, 12 and 24 h. After this time, samples (50-250 µL) were withdrawn every 24 h up to 168 h. The total volume of the 16 samples did not exceed 2.9% of the initial solution volume.

The influence of initial solution pH on P removal was examined at initial P concentration of 10 mg/L. The initial pH was adjusted to the desired values (ranging from 4 to 9) using HCl and/or NaOH before adding the adsorbent. After equilibration of 120 h at 298 K, the final solution pH was also measured.

Equilibrium experiments were carried out for 120 h at 288, 298 and 308 K using five low initial P concentrations (0.5, 1, 2, 5 and 10 mg/L) at pH 7. Isotherm models were applied at higher initial P concentrations (25, 50, 75, 100 and 200 mg/L) under the same experimental conditions. The adsorption capacity of CaT-Z for PO<sub>4</sub>-P at time  $t$  and equilibrium,  $q_t$  and  $q_e$  (mg/g), respectively, was calculated with the following equations:

$$q_t = (C_0 - C_t)V/m \quad (1)$$

$$q_e = (C_0 - C_e)V/m \quad (2)$$

where  $C_0$ ,  $C_e$  and  $C_t$  are the initial P concentration, the P concentration at equilibrium and at time  $t$  (mg/L), respectively;  $V$  is the volume of the working solution (L) and  $m$  is the adsorbent mass (g).

The removal efficiency ( $R\%$ ) of CaT-Z for PO<sub>4</sub>-P was calculated by Eq. (3):

$$R(\%) = 100 \times (C_0 - C_e)/C_0 \quad (3)$$

The effect of various individual co-existing ions on the PO<sub>4</sub>-P sorption was studied in 20 mL solutions containing 10 mg P/L and 0.01 M of the following salts: KNO<sub>3</sub>, NaHCO<sub>3</sub>, NaCl, K<sub>2</sub>SO<sub>4</sub>, NH<sub>4</sub>Cl, sodium acetate (CH<sub>3</sub>COONa), sodium citrate monobasic (C<sub>6</sub>H<sub>7</sub>O<sub>7</sub>Na) or 0.001 M sodium dodecyl sulphate [SDS: CH<sub>3</sub>(CH<sub>2</sub>)<sub>11</sub>OSO<sub>3</sub>Na]. These tests were conducted for 120 h at pH 7 and 298 K. The same experimental conditions were performed to evaluate the effect of organic matter (10 and 50 mg/L humic acid). In addition, the influence of Ca<sup>2+</sup>

(pH 7),  $Mg^{2+}$  (pH 7) and  $Fe^{2+}$  (pH 5.5) on sorption removal (10 mg P/L) were investigated at three different cation concentrations (10, 50 and 100 mg/L) using  $CaCl_2 \cdot 2H_2O$ ,  $MgSO_4 \cdot 7H_2O$  and  $FeSO_4 \cdot 7H_2O$ .

#### 2.4. Desorption study

Desorption tests were carried out to determine the phosphate adsorption mechanisms and binding forms on the adsorbent. Three different  $PO_4$ -P fractions bound on the P-loaded CaT-Z were measured by a sequential extraction procedure [3]. Equilibrated samples (100 mg) of CaT-Z loaded with 10 and 100 mg P/L during the isotherm test at 298 K were extracted by 10 mL eluent. The eluents used sequentially for 24 h were 0.5 M  $NaHCO_3$  (pH 8.5), 1 M NaOH and 0.5 HCl. After each extraction step the sorbent was washed four times with DI remaining in the bottle and then dried at 343 K overnight.

The desorption efficiency of each step was calculated by the following equation:

$$Desorption (\%) = 100 \times (q_{des}/q_{ads}) \quad (4)$$

where  $q_{des} = (C_{des} V/m)$  and  $q_{ads}$  (Eq. 2) are the desorption and adsorption capacity (mg P/g) at equilibrium, respectively, and  $C_{des}$  (mg/L) is the liquid phase P concentration in the desorbing solution [32].

#### 2.5. Adsorption models

The kinetic data were fitted to chemical reaction (pseudo-first order, pseudo-second order and Elovich) and to diffusion based models (Weber-Morris and Reichenberg

intraparticle diffusion models). The isotherm models of Langmuir, Freundlich, Temkin and Koble-Corrigan were applied to equilibrium data for initial P concentrations in the range of 25-200 mg/L. The linear forms of the kinetic and isotherm models are given in Supplementary material (Adsorption models). The fit goodness of the isotherm and kinetic models to the experimental data was evaluated by the coefficient of determination ( $R^2$ ) using linear regression analysis and the root mean square error (RMSE) (see Supplementary material).

### 3. Results and discussion

#### 3.1. Effect of $\text{Ca(OH)}_2$ treatment on phosphate removal

Fig. 1 shows that the pretreatment of NZ with  $\text{Ca(OH)}_2 \geq 0.1 \text{ M}$  resulted in a significant increase of P removal ( $R\%$ ) for both low and high initial P concentration. The removal of P by NZ was very low. At 10 mg P/L, the NZ pretreatment with 0.1 M  $\text{Ca(OH)}_2$  led to a  $R\%$  increase from 1.7% (NZ) to 94.8% (CaT-Z), whereas the  $R\%$  of CaT-Z (ranged in 93.5-94.8%) was not significantly affected by the increase of  $\text{Ca(OH)}_2$  concentration up to 1 M. This result is due to the available and unsaturated binding sites on CaT-Z surface at low P concentrations [33]. In the case of 100 mg P/L and NZ pretreatment with 0.1 M  $\text{Ca(OH)}_2$ , CaT-Z provided a  $R\%$  of 67.8%, whereas NZ adsorbed no P (zero  $R\%$ ). The  $R\%$  reduced from 67.8 to 61.9% with the increase of  $\text{Ca(OH)}_2$  up to 1 M (Fig. 1). The  $R\%$  decrease can be attributed to the precipitation and aggregation of  $\text{Ca(OH)}_2$  particles at higher molarity due to its low water solubility, i.e. 0.018 M at 23 °C [34], resulting in clogging of NZ pores and hindered diffusion of  $\text{Ca(OH)}_2$  into internal surface binding sites.

A cost-effective pretreatment of NZ by using **small amounts of** chemicals for its surface modification is desired. **Thus**, the NZ modification with 0.25 M Ca(OH)<sub>2</sub> was selected for further sorption tests as it showed minor *R*% difference (-2.95% at 100 mg P/L) from the respective one at 0.1 M Ca(OH)<sub>2</sub>.

## **3.2. Characterization of adsorbent**

### **3.2.1. SEM-EDS analysis**

The surface of NZ and CaT-Z was investigated by using the SEM technique (**Fig. 2a and b**). The untreated and pretreated material revealed a very rough and heterogeneous surface characterized by the predominant mineral clinoptilolite and dispersed igneous relics like anorthitic plagioclase. **Compact hydrated layer on CaT-Z surface after reaction of NZ with Ca(OH)<sub>2</sub> was not observed, even at high magnification.** The latter is in contrast with our previous findings [23] where the Ca(OH)<sub>2</sub> reacted with the montmorillonite matrix forming a well compacted thin layer. We have observed, however, an increased CaO content (44-65 wt% based on dry weight) on the CaT-Z surface in contrast to the negligible amount of NZ, as it is clearly illustrated in the respective EDS analysis (EDS spectra A and B are given in **Supplementary Material: Fig. S1**).

**The presence of phosphorus in the form of apatite [calcium phosphate - Ca<sub>5</sub>(PO<sub>4</sub>)<sub>3</sub>(OH,F,Cl)] was verified** occurring as well compacted thin layer and needle-like (fibrous) crystals (< 5 μm in diameter) **in the P loaded CaT-Z (Fig. 2c and d). Apatite composition was also verified by** using EDS (34-41% dry weight as P<sub>2</sub>O<sub>5</sub>; see also EDS spectra C and D in Supplementary Material: **Fig. S1**). The formation of apatite as the most

thermodynamically stable Ca-P precipitate may occur at pH range 7.0-9.0 when the molar ratio of  $\text{Ca}/\text{PO}_4^{3-}$  in the solution is  $> 1.67$  [3, 21].

### 3.2.2. XRD analysis

The XRD patterns of NZ, CaT-Z and P-loaded CaT-Z are given in **Fig. 3**. The untreated NZ is composed by the mineral assemblage clinoptilolite, illite, plagioclase (mainly anorthite), potassium feldspar, and montmorillonite.

The CaT-Z XRD pattern is similar to the untreated one, but without the montmorillonite peak at  $\sim 15\text{\AA}$  and also none of the observed peaks related to  $\text{Ca}(\text{OH})_2$ . In the P-loaded CaT-Z at both P concentrations of 10 and 100 mg/L, clinoptilolite, illite, anorthite, potassium feldspar were also detected. Additionally, in the case of CaT-Z loaded with 100 mg P/L, the XRD pattern probably reveals a potassium-phosphorus-bearing phase (K-P) at  $21^\circ$ . The formation of this phase can be related to the significant reduction of  $\text{K}^+$  concentration in sorption solution by 59.4% observed after 120 h, i.e. from 128.33 to 52.08 mg/L. The exchangeable  $\text{K}^+$  and  $\text{H}^+$  cations obtained by the dissociation of  $\text{KH}_2\text{PO}_4$  reagent used for the sorption solution can be adsorbed in the zeolite aluminosilicate framework. In particular, the zeolite acting as “molecular sieve” may accept only molecules smaller than its pore diameter. Given the smaller ionic diameter ( $6.6\text{\AA}$ ) of the hydrated  $\text{K}^+$  compared to the zeolite structure (mesoporous ca. 20-500  $\text{\AA}$  and microporous ca.  $<20\text{\AA}$  in diameter) and the preferential selectivity of clinoptilolite for  $\text{K}^+$  (via cation exchange with other adsorbed cations such as  $\text{Ca}^{2+}$  [35, 36]), the inward diffusion of  $\text{K}^+$  through the pore channels is possible. Despite the applied pretreatment with  $\text{Ca}(\text{OH})_2$ ,

however, the CaT-Z retained its cation exchange sites. Therefore, the adsorbed  $K^+$  cations might interact further with phosphate anions, which were migrated in the interior of CaT-Z. This interaction can take place through the coordination of the monovalent anion  $[H_2PO_4]^-$  inside the zeolite cavities with the adsorbed  $K^+$  cations forming two hydrogen bonds with a zeolite framework oxygen atom (Al-O-Si) [37]. Furthermore, the apatite or other Ca-P phases were not detected either at 10 or 100 mg P/L experiment (Fig. 3). As long as the apatite phase was observed in SEM (Fig. 2c and d), it suggests that the modal content was below the detection limit of XRD.

### 3.2.3. IR-ATR analysis

Representative IR-ATR spectra of the NZ, CaT-Z and P-loaded CaT-Z are shown in Fig. 4. The IR spectrum of the NZ exhibits a band at  $\sim 1019\text{ cm}^{-1}$ , as well as shoulders at  $\sim 1130$  and  $\sim 1204\text{ cm}^{-1}$  which can be assigned to a convolution of the Si-O-Si asymmetric stretching vibrations in the silicate minerals detected by XRD (Fig. 3). The  $790\text{ cm}^{-1}$  band can be attributed to the Si-O-Si bridge bending in corner-sharing  $SiO_4$  tetrahedra [38]. The  $596\text{ cm}^{-1}$  band could tentatively be attributed to stretching vibrations of aluminate octahedra [39], associated with the plagioclase or the potassium feldspar. The  $1630\text{ cm}^{-1}$  band originates from the H-O-H bending vibrations of water molecules incorporated in hydrated minerals (e.g., montmorillonite). The OH stretching vibration envelope  $3000\text{--}3700\text{ cm}^{-1}$  is a convolution of the hydroxyl vibrations belonging to either water molecules or structural hydroxyl groups [39]; nevertheless, the narrow  $3615\text{ cm}^{-1}$  band must be related to a characteristic structural OH containing mineral like illite [40].



The IR spectrum of the CaT-Z sample exhibits notable differences compared to that of the NZ; new sharp IR bands were observed at 858 and 875  $\text{cm}^{-1}$  in addition to the broad 1400-1580  $\text{cm}^{-1}$  envelope. Here, we attempt to infer constraints on the origin of the former peaks. Initially, we consider that the new peak at 875  $\text{cm}^{-1}$  could be related to the 871  $\text{cm}^{-1}$  peak measured in the infrared spectrum of  $\text{Ca}(\text{OH})_2$  suggesting incorporation of hydrated lime in the starting material [22]. The 871  $\text{cm}^{-1}$  peak in turn is commonly associated with a strong and narrow OH stretching band at 3641  $\text{cm}^{-1}$  [22], which is not observed in Fig.4. In contrast, the 3615  $\text{cm}^{-1}$  band is present already in the spectrum of the NZ. Therefore, the infrared spectroscopy, in agreement with XRD results, suggests that no  $\text{Ca}(\text{OH})_2$  is present in the CaT-Z sample studied here.

After that, we infer that the new IR peaks of the CaT-Z sample should be associated with the conversion of the  $\text{Ca}(\text{OH})_2$  to  $\text{CaCO}_3$  by chemisorption of atmospheric  $\text{CO}_2$  on the  $\text{Ca}(\text{OH})_2$  surface [22, 41]. Carbonate anions ( $\text{CO}_3^{2-}$ ) of  $D_{3h}$  symmetry exhibit in the infrared three modes; the in-plane bend at ca. 700  $\text{cm}^{-1}$  ( $\nu_4$ ), the out-of-plane bend at ca. 870  $\text{cm}^{-1}$  ( $\nu_2$ ), and the asymmetric stretch in the 1400-1600  $\text{cm}^{-1}$  ( $\nu_3$ ) range [42]. Inspection of the CaT-Z spectrum in Fig. 4 shows very weak absorption in the region of  $\nu_4$  and two well-separated peaks at 858 and 875  $\text{cm}^{-1}$  in the region of  $\nu_2$ , while the region of  $\nu_3$  shows features at 1420  $\text{cm}^{-1}$  (weak), 1474  $\text{cm}^{-1}$  (strong) and 1525  $\text{cm}^{-1}$  of medium intensity. These results show that  $\text{Ca}(\text{OH})_2$  was converted to  $\text{CaCO}_3$ , probably with different crystal structure, following the reaction [41]:  $\text{Ca}(\text{OH})_2 + \text{CO}_2 \rightarrow \text{CaCO}_3 + \text{H}_2\text{O}$ . The 858  $\text{cm}^{-1}$  peak of CaT-Z could be related to  $\nu_2$  of aragonite and the one at 875  $\text{cm}^{-1}$  to  $\nu_2$  of calcite [43]. The strongest components of  $\nu_3$  were measured at 1475  $\text{cm}^{-1}$  for aragonite and at 1430

cm<sup>-1</sup> for calcite [43] in good agreement with the profile of the  $\nu_3$  region of CaT-Z in **Fig. 4**. As found here the new bands of CaT-Z confirm the modification of zeolite surface after its pretreatment with the hydrated lime.

The IR response of the low concentration P-loaded CaT-Z material is quite similar to the CaT-Z one. However, the intensity of the broad envelope at 1475 cm<sup>-1</sup> and those of the narrow peaks at 858 and 875 cm<sup>-1</sup> all decrease after the adsorption of 10 mg P/L, and then they are eliminated at the higher P concentration of 100 mg P/L (**Fig. 4**). These changes are most likely attributed to a ligand exchange mechanism between solution phosphate anions and CaT-Z surface CO<sub>3</sub><sup>2-</sup> and OH<sup>-</sup> groups. We have recently observed similar IR-ATR features after phosphate adsorption onto Ca(OH)<sub>2</sub> treated bentonite [23]. The peak at ca. 875 cm<sup>-1</sup> in the spectrum of 100 mg P/L loaded CaT-Z should not be related to the presence of carbonates, as the stronger ~1475 cm<sup>-1</sup> carbonate band has almost disappeared. This peak has a linewidth similar to the shoulder visible in the NZ spectrum in the same frequency region. Minor differences were observed in the region of Si-O-Si stretching after Ca(OH)<sub>2</sub> treatment and P adsorption; the 1019 cm<sup>-1</sup> band downshifts slightly to 1012 cm<sup>-1</sup> while the lower-intensity shoulders at ca. 1130 and 1205 cm<sup>-1</sup> did not show any appreciable shifting. However, we were unable to detect separate bands in the two P-loaded CaT-Z samples that may suggest the presence of orthophosphate anions (PO<sub>4</sub><sup>3-</sup>). The theoretical infrared response of tetrahedral PO<sub>4</sub><sup>3-</sup> anions is dominated by the asymmetric stretch mode around 960 cm<sup>-1</sup> and the bend mode at ca. 550 cm<sup>-1</sup> [44]. In our samples, the presence of PO<sub>4</sub><sup>3-</sup> anions seems to be associated with the downshift of the main infrared band to 1012 cm<sup>-1</sup> and the appearance of the ca. 560 cm<sup>-1</sup> shoulder in the

spectrum of the 100 mg P/L loaded CaT-Z (**Fig. 4**). Based on the previous infrared features, we conclude that only a minor amount of phosphate has been formed.

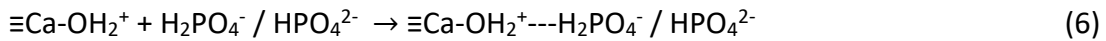
#### 3.2.4. Determination of surface point of zero charge

The electrical charge of natural zeolite surface depends on the permanent negative charge of their aluminosilicate framework due to isomorphous substitution of aluminium ( $\text{Al}^{3+}$ ) for silicon ( $\text{Si}^{4+}$ ) [5, 45] and on the solution pH, which influences the protonation/deprotonation of the surface functional groups. Modification of the surface functional groups by chemical pretreatment of the raw mineral can change the value of  $\text{pH}_{\text{pzc}}$ . [45] As shown in **Fig. 5a**, the  $\text{pH}_{\text{pzc}}$  values of NZ and CaT-Z were determined by the intersection of the  $\Delta\text{pH}$  linear plots ( $R^2 > 0.948$ ) with the x-axis. The results indicated that the chemical pretreatment of NZ with  $\text{Ca}(\text{OH})_2$  caused a significant increase of  $\text{pH}_{\text{pzc}}$  changing the acidic surface of NZ ( $\text{pH}_{\text{pzc}} \approx 6.14$ ) to basic one for CaT-Z ( $\text{pH}_{\text{pzc}} \approx 9.98$ ). This improvement of  $\text{pH}_{\text{pzc}}$  suggests the formation of hydroxyl and carbonate ligands on the CaT-Z surface [20]. An improved  $\text{pH}_{\text{pzc}}$  was also observed after the pretreatment of bentonite with 1 M  $\text{Ca}(\text{OH})_2$  [23].

#### 3.3. Influence of solution pH

At solution pH value equal to  $\text{pH}_{\text{pzc}}$  the adsorbent surface is electrically neutral, while at  $\text{pH} < \text{pH}_{\text{pzc}}$  the adsorbent surface is positively charged. In the examined initial pH range of 4-9 (**Fig. 5b**), the CaT-Z surface was protonated and carried positive charge, while the dominant phosphate species in the solution were the monovalent  $\text{H}_2\text{PO}_4^-$  at  $\text{pH} < 7.2$

( $pK_1 = 2.15$ ) and the divalent  $HPO_4^{2-}$  anion at  $pH \geq 7.2$  ( $pK_2 = 7.20$ ) [4, 7]. The net positive charge of CaT-Z surface at these pH values favoured the electrostatic forces of attraction for both phosphate species. The formation of outer-sphere surface complexes between  $H_2PO_4^-$  or  $HPO_4^{2-}$  and CaT-Z surface (Eq. 6) can occur at acidic pH when surface  $OH^-$  groups are protonated according to Eq. 5 [46, 47]:



As shown in **Fig. 5b**, the increase of initial solution pH from 4 to 9 did not affect the  $PO_4$ -P removal ( $R\%$ ) by CaT-Z. This pH-independency of  $R\%$  is an indication of specific adsorption mechanism [4]. Besides, the final solution pH after 120 h of adsorption process increased with increasing initial pH reaching values from 8.46 to 9.60 which were lower than  $pH_{pzc}$ . The increase of solution pH which also led to a decrease of  $pH_{pzc}$  from 9.98 to about 8.79 after phosphate loading on CaT-Z (**Fig. 5a**) indicated the dominant role of the ligand exchange mechanism [4, 48]. During the ligand exchange, monovalent and bivalent phosphate anions replaced  $OH^-$  groups located on the CaT-Z surface, as confirmed by the IR-ATR study (**Fig. 4**, where the  $OH^-$  stretching envelope intensity is reduced for the loaded CaT-Z samples), and formed inner-sphere surface complexes via Lewis acid-base interactions between phosphate and  $\equiv Ca-OH$  groups as expressed by Eq. 7 and 8. [7]. As a result, hydroxyl groups were released to the solution and caused the pH increase [6]. The inner-sphere complexes can be both monodentate and bidentate complexes between

the unprotonated phosphate oxygen atoms and the  $\equiv\text{Ca-OH}$  functional groups. Phosphate anions behave like Lewis bases donating electron pair(s) by binding to Ca atom [6]. On the other hand, the decreasing P adsorption via electrostatic attraction (outer-sphere complexation) with increasing pH, as the CaT-Z surface charge became less positive, was counterbalanced by the favoured calcium phosphate precipitation on CaT-Z surface at pH 7-9. The pH-independent removal efficiency of CaT-Z observed in this study is a benefit for phosphate removal under acidic and alkaline conditions. Usually, the pH of municipal wastewater ranges from 6.5 to 7.3 [6, 10] while that of eutrophic lakes is 8-9 [11]. Moreover, it is not necessary to adjust the solution or wastewater pH, thus reducing the use of reagents and so the operational costs in practical applications.



### 3.4. Effect of contact time

**Fig. 6** shows the change of  $\text{PO}_4\text{-P}$  removal versus time at two different initial P concentrations. It was observed that the equilibrium of  $\text{PO}_4\text{-P}$  adsorption onto CaT-Z was reached at 120 h for 10 mg P/L and after 168 h for 100 mg P/L, presenting a 96.9% and 66% removal efficiency up to 168 h, respectively. The parameters of the reaction based kinetic models are summarized in **Table S1**. The  $\text{PO}_4\text{-P}$  adsorption was a slow process (**Fig. 6**) and the half of adsorption capacity was achieved after 8.5 and 18 h ( $t_{1/2}$ ) for 10 and 100 mg P/L, respectively (**Table S1**). The slow kinetics of phosphate sorption onto CaT-Z is

consistent with the reports of Yin et al [9, 20] for calcium-rich adsorbents which generally require days to achieve equilibrium for P removal. However, the P removal rate can be enhanced by increasing the CaT-Z dosage.

In the case of 10 mg P/L, the pseudo-second order equation fitted the kinetic data better than the pseudo-first order model **resulted in** higher  $R^2$  and lower  $RMSE$  values and **thus** the calculated adsorption capacity ( $q_{e,cal}$ ) was much closer to the experimental one ( $q_{e,exp}$ ) (**Table S1**). At 100 mg P/L, both pseudo-first and pseudo-second order model showed a high  $R^2$  ( $> 0.985$ ) and similar difference of  $q_{e,cal}$  from the  $q_{e,exp}$  indicating a complicated adsorption mechanism. However, the pseudo-second order model provided a lower  $RMSE$  value (**Table S1**). The adsorption rate constants  $k_1$  and  $k_2$  decreased with the increase of the initial P concentration suggesting that more time is required to achieve equilibrium at higher solute concentrations. In contrast, the initial adsorption rate  $h$  of the pseudo-second order model which corresponds to surface sorption sites, increased due to a higher driving force at higher P concentrations. The Elovich model **exhibited** lower  $R^2$  values than those of the other two reaction kinetic models but lower  $RMSE$  values than those of the pseudo-first order model. Thus, the pseudo-second order kinetic model best matched the entire time data due to high  $R^2$  and lower  $RMSE$  values than those of the pseudo-first order model, suggesting a chemisorption mechanism involving valency forces via sharing or exchanging electrons [22]. Similar kinetic results were reported for phosphate adsorption onto Zr-modified zeolite [16] and Fe-modified bentonite [11].

Because the chemical reaction kinetic models assume only one mechanism [49], a further analysis of kinetic data by diffusion based models was performed. **Fig. S2a and b**

show the plots of  $q_t$  versus  $t^{0.5}$  at 10 and 100 mg P/L, which presented a multilinearity with three distinct kinetic steps. The initial steeper step was completed in the first 24 h for both initial P concentrations with  $R^2 > 0.981$  (Table S1) and represented the external mass transfer (film diffusion) of phosphate anions from bulk solution to the boundary layer surrounding the CaT-Z particles. The intermediate linear part, lasted from 24-72 and 24-120 h for 10 and 100 mg P/L respectively, corresponded to the intraparticle diffusion of phosphate into the clinoptilolite pores [50]. As can be seen in Table S1, the diffusion rate reduced with the contact time ( $k_{ip1} > k_{ip2} > k_{ip3}$ ) since equilibrium was gradually reached up to 168 h as presented by the third linear part of Weber-Morris plot. The non-zero values of  $I$  suggested that the intraparticle (pore) diffusion was not the only rate-limiting mechanism during P adsorption onto CaT-Z.

The pore diffusion model of Reichenberg (Eq. S8) was applied at the initial stage of the adsorption (for 0-24 and 0-96 h at 10 and 100 mg P/L, respectively) giving high  $R^2$  values for both initial P concentrations (Fig. S2c, Table S1). The effective pore diffusion coefficient ( $D_{eff}$ ) decreased with increasing  $C_0$ , i.e. from  $7.62 \times 10^{-13}$  to  $2.37 \times 10^{-13}$  m<sup>2</sup>/s, indicating a more effective phosphate diffusion at 10 mg P/L (Table S1). The regression lines of Reichenberg plot did not pass through the origin (intercept = -0.0482 and -0.0129) suggesting that film diffusion affected the phosphate adsorption kinetics at the initial stage of the process [51].

### 3.5. Effect of low initial P concentrations

The effect of low initial P concentrations ( $\leq 10$  mg/L) on P removal and equilibrium P concentration at different temperatures is presented in **Fig. 7a** and **b**. According to the experimental results, the CaT-Z exhibited a high affinity for phosphate anions at low P concentrations which can be found in effluents of domestic wastewater treatment. The P removal efficiency ( $R\%$ ) at 298 K increased from 83.9 to 97.6% when the initial P concentration increased from 0.5 to 10 mg/L (**Fig. 7a**), while the  $R\%$  increased from 35 to 90.5% at 288 K and from 82.9 to 99.2% at 308 K. The increased  $R\%$  with rising temperature suggests an endothermic nature of  $\text{PO}_4\text{-P}$  adsorption onto CaT-Z. Therefore, adsorption by using CaT-Z showed a high phosphate removal efficiency at low P concentrations where chemical precipitation and biological removal are not effective as wastewater treatment methods [2, 4]. After 120 h of sorption process, the range of the residual P concentration in the solution was 0.325-0.962, 0.081-0.238 and 0.047-0.079 mg/L at 288, 298 and 308 K, respectively (**Fig. 7b**). These P concentrations are consistent with the European Union requirements ( $< 1\text{-}2$  mg P/L) for effluent discharges from municipal wastewater treatment plants to sensitive areas (Directive 98/15/EC) [13]. This result is important due to the need for wastewater treatment effluents with very low phosphate concentrations [4].

### 3.6. Adsorption isotherms

Batch adsorption studies were also conducted at three different temperatures with higher  $\text{PO}_4\text{-P}$  concentrations (25-200 mg/L) which can be found in agricultural wastewater or anaerobic fermentation liquor [25, 52]. As shown in **Fig. 8**, the  $q_e$  of CaT-Z for  $\text{PO}_4\text{-P}$  increased with the rising initial P concentration and solution temperature (288-308 K)



indicating an endothermic process. The increase of  $q_e$  with temperature is probably attributed to enhanced diffusion of phosphate anions into the smaller micropores of CaT-Z and thus accessing more binding sites [2, 11]. As expected, the  $R\%$  decreased (i.e. from 91.6 to 37.9% at 298 K) when the P concentration increased in the range of 25-200 mg/L at all studied temperatures (data not shown).

The isotherm model parameters estimated through the linear regression method ( $R^2$ ) and the values of the statistical error  $RMSE$  are listed in **Table 1**. The comparison of the two-parameter isotherm models showed that the Langmuir model provided the best fit to the experimental data at 288 and 308 K ( $R^2 \geq 0.970$  and  $RMSE \leq 0.78$ ), whereas Freundlich isotherm ( $R^2 = 0.976$  and  $RMSE = 0.32$ ) described better the adsorption of  $PO_4$ -P at 298 K followed by Temkin equation ( $R^2 = 0.963$  and  $RMSE = 0.34$ ). Freundlich and Temkin models describe heterogeneous adsorption systems [53].

Although Langmuir model also showed a satisfactory correlation with data at 298 K, the calculated  $q_{max}$  underestimated the experimental value of  $q_e$  (7.57 mg P/g at  $C_0 = 200$  mg P/L) and did not follow the increasing trend of  $q_e$  with temperature. The favorable  $PO_4$ -P adsorption onto CaT-Z was confirmed at all studied temperatures as the values of the dimensionless separation factor  $R_L$  (obtained by the Langmuir constant  $b$ ) and the Freundlich constant  $n$  are within the favorable equilibrium ranges ( $0 < R_L < 1$  and  $n > 1$ ).

The good fitting of Langmuir isotherm at 288 and 308 K, assuming a monolayer  $PO_4$ -P adsorption on homogeneous surface, might be due to the modification of NZ by  $Ca(OH)_2$  which partially changed its heterogeneous surface by creating homogeneous surface regions with finite number of binding sites for  $PO_4$ -P adsorption. On the other hand, the

good fit of Freundlich equation at 298 K which assumes multilayer adsorption on heterogeneous surfaces taking into account the sorbent-sorbate interactions, can be related to the multilayer Ca-P precipitates [20] confirmed by the SEM images (**Fig. 2d**).

At 288 and 308 K, the three-parameter isotherm model of Koble-Corrigan fitted the experimental data better than the two-parameter models presenting a favorable adsorption ( $n > 1$ ), the highest  $R^2$  ( $\geq 0.982$ ) and low  $RMSE$  values ( $\leq 0.96$ ). The Koble-Corrigan model could not describe the experimental data at 298 K, despite the highest  $R^2$ , because the value of  $n$  was found to be lower than 1 (**Table 1**). As combined form of Langmuir and Freundlich models, the Koble-Corrigan isotherm can better fit the experimental data for both low and high solute concentrations [33]. This model is used for heterogeneous adsorption surfaces and is transformed to Langmuir isotherm when  $n = 1$  [54]. The  $n$  values at 288 and 308 K suggested an adsorption reaction stoichiometry of more than 1 solute molecule per free sorbent binding site [55]. Therefore, the best applicability of Langmuir and Koble-Corrigan isotherms at 288 and 308 K suggested a complex adsorption mechanism with heterogeneous and homogeneous uptakes of  $PO_4\text{-P}$  by CaT-Z.

The CaT-Z exhibited a satisfactory and comparable P adsorption capacity to that of other modified mineral adsorbents reported in **Table S2**, although it was lower than that of the  $Ca(OH)_2$  treated bentonite. The comparison in **Table S2** should also take into account the particle size of the listed adsorbents which mostly were fine powders with a higher specific surface area than that of CaT-Z. The good removal efficiency at both low and high P concentrations, despite the larger particle size, and the low cost and eco-

friendly pretreatment of CaT-Z render this material as an efficient adsorbent for use in water/wastewater purification. Regarding the separation of the adsorbent from the liquid phase, the application of powder sorbents or pure metal oxides/hydroxides in wastewater treatment is less practical [4, 7, 16], despite their high P adsorption capacity.

### 3.7. Effect of coexisting ions and organic matter

Natural aquatic ecosystems and real wastewaters contain several ions which can compete with phosphate for binding sites on the adsorbent surface. Fig. 9a presents the effect of inorganic and organic substances at concentration 31-fold (or 3-fold in the case of SDS surfactant) higher than that of PO<sub>4</sub>-P (10 mg P/L = 0.323 mmol P/L). It was observed that the presence of NO<sub>3</sub><sup>-</sup>, Cl<sup>-</sup> and NH<sub>4</sub><sup>+</sup> in the sorption solution did not significantly affect the R% of PO<sub>4</sub>-P (95.2-98.7%) compared to the solution containing only PO<sub>4</sub>-P (98%). The presence of the other coexisting substances exhibited a more negative effect on P removal, following the order: SO<sub>4</sub><sup>2-</sup> (89.9%) > SDS (84.5%) > HCO<sub>3</sub><sup>-</sup> (71.1%) > acetate (44.5%) > citrate (31.4%) (Fig. 9a). The organic oxyanions acetate and citrate showed the highest competing effect on R% due to competition with phosphate for binding sites [56]. The negative effect of citrate anion was much higher than that of acetate because the first contains more carboxylic groups (three) than acetate (one) [52].

The anions NO<sub>3</sub><sup>-</sup>, SO<sub>4</sub><sup>2-</sup> and Cl<sup>-</sup> are non-specifically adsorbed forming outer-sphere surface complexes and exhibiting little influence on phosphate sorption [4, 6]. Phosphate removal by natural zeolite can be even enhanced by the presence of NH<sub>4</sub><sup>+</sup>. The ion exchange between solution NH<sub>4</sub><sup>+</sup> and surface bound Ca<sup>2+</sup> can cause the surface

precipitation of the dissolved phosphate by the formation of amorphous calcium phosphate in the liquid phase [25, 52]. A similar process is possible in the present work, since the release of  $\text{Ca}^{2+}$  from  $\text{Ca}(\text{OH})_2$  treated bentonite into the solution was observed during phosphate adsorption [23]. On the other hand, the decrease of  $R\%$  by 28% in the presence of  $\text{HCO}_3^-$  is due to the specific adsorption of carbonates forming inner-sphere complexes **with  $\text{Ca}^{2+}$  hindering** the formation of calcium phosphate precipitates on CaT-Z surface [3]. A negative effect of  $\text{HCO}_3^-$  on phosphate adsorption was also observed **in the case of** other modified mineral adsorbents [9, 20, 52].

The removal of  $\text{PO}_4\text{-P}$  by CaT-Z was also tested in the presence of dissolved organic matter. Humic acid (HA) is produced from the degradation of organic matter and plant roots secretion [9] and has been used to simulate natural organic matter in the secondary effluents of wastewater treatment plants [56]. **Fig. 9b** shows that HA at medium (10 mg/L) and high (50 mg/L) concentrations presented a very low competitive effect on  $\text{PO}_4\text{-P}$  removal (a 6.4% decrease of  $R\%$  at 50 mg HA/L). Similar result was reported for phosphate adsorption on magnetite core/zirconia shell nanoparticle material [56].

The good selectivity of CaT-Z for low P concentrations even in the presence of other anions suggests a benefit for its practical use as adsorbent. **It should be noted** that the concentration levels of the **tested** anions in natural water or wastewater are much lower than these used in this work, so their competing effect on phosphate adsorption **is expected to be even** lower. When ionic strength does not influence the adsorption process, then the inner-sphere complexation is important as adsorption mechanism [49]

suggesting that phosphate were linked with strong (i.e. covalent) bonds with adsorption sites of CaT-Z.

**Fig. 9b** presents the effect of liquid phase calcium (pH 7), magnesium (pH 7) and ferrous iron (pH 5.5) at three different concentrations on PO<sub>4</sub>-P removal efficiency. It was observed that Ca<sup>2+</sup> had no significant effect on *R*%, whereas the presence of Mg<sup>2+</sup> caused a slight *R*% decrease by 4-10.5%. In contrast, the PO<sub>4</sub>-P removal by CaT-Z significantly decreased by the presence of Fe<sup>2+</sup> (**Fig. 9b**). This decrease was attributed to the phosphate adsorption or incorporation in iron oxyhydroxide colloids [57]. The initial pH of sorption solution containing Fe<sup>2+</sup> was chosen to be acidic (5.5) in order to simulate acidic soils where P is immobilized by Fe and Al oxides [58]. However, it was observed that the final solution pH altered to basic values (8.5-9.4) due to the effect of ligand exchange mechanism. It is known that at pH > 7, aqueous Fe<sup>2+</sup> (as dissolved FeSO<sub>4</sub> · 7H<sub>2</sub>O) can be oxidized to Fe<sup>3+</sup> [57] which interacts with water molecules forming hydrolysis products such as Fe(OH)<sup>2+</sup>, Fe(OH)<sub>2</sub><sup>+</sup>, Fe<sub>2</sub>(OH)<sub>2</sub><sup>4+</sup> etc [59]. These products can then interact with oxoanions such as PO<sub>4</sub><sup>3-</sup> through electrostatic adsorption, surface complexation and co-precipitation [59]. The formation of soluble Fe-P complexes caused the decrease of *R*% by CaT-Z. Iron (hydro)oxides also occur in natural water bodies, but in much lower concentrations than these tested here, presenting a strong affinity for phosphate [60].

### 3.8. Sequential desorption study

**Fig. 10** shows the results of the sequential extraction of adsorbed P from the loaded CaT-Z using NaHCO<sub>3</sub>, NaOH and HCl solutions. These eluents correspond to the

weakly (loosely) bound P, Al- and Fe- associated P, and Ca bound P (Ca-P), respectively [3, 19]. The total amount of P extracted from the loaded CaT-Z at the three steps was 85.9 and 96.3% of  $q_{e,ads}$  at 10 and 100 mg P/L, respectively. In the case of 10 mg P/L, the major fractions of P were found to be the Ca-P (39.8%) and P associated to Al oxides/hydroxides (37.2%) since CaT-Z did not contained Fe according to SEM-EDS analysis. The weakly bound P fraction ( $\text{NaHCO}_3\text{-P}$ ) was minor (8.9%), representing weak outer-sphere complexes through electrostatic bonding between phosphate and surface protonated hydroxyl groups. On the other hand, the CaT-Z loading at 100 mg P/L enhanced the predominant speciation of Ca-P (HCl-P) to 85.3% due to favored surface precipitation of Ca-P compounds at higher P concentrations as continuation of surface complexation [21]. The P immobilization due to Al-P form drastically decreased (1.4%) and the loosely bound P fraction did not significantly change (9.6%) compared to that at 10 mg P/L (**Fig. 10**). The NaOH extractable P represents a speciation of inner-sphere surface complexation [19] which is considered algal available and released under anoxic conditions at sediment-water interface [61]. This P fraction is sensitive to high pH (exchangeable with  $\text{OH}^-$ ) while HCl extractable P represents P sensitive to low pH. Thus, the release of NaOH-P and HCl-P forms under natural water conditions (pH 5-9) is impossible, and these adsorbed P forms are considered to be relatively stable [16].

#### 4. Conclusions

After modification of natural zeolite (clinoptilolite) with  $\text{Ca}(\text{OH})_2$ , a significant improvement of  $\text{PO}_4\text{-P}$  adsorption from aqueous solutions was observed. The CaT-Z

provided a high P removal efficiency at low initial P concentrations (0.5-10 mg/L), typical for domestic wastewater treatment effluents, leading to low residual concentrations at ppb level ( $\mu\text{g/L}$ ), which satisfy the European Union standards for tertiary wastewater treatment. The good adsorption capacity (7.57 mg P/g) at higher P concentration (200 mg/L) suggested a beneficial use of CaT-Z for agricultural wastewater treatment such as digestion or fermentation effluents. The porous structure of CaT-Z and the slow P adsorption kinetics due to intra-particle diffusion make CaT-Z a promising novel filter medium for long-term P removal in constructed wetlands. In the range of 25-200 mg P/L, the equilibrium data were best fitted by Freundlich model at 298 K and by Koble-Corrigan model at 288 and 308 K indicating a phosphate adsorption on heterogeneous surface. The CaT-Z exhibited a high selectivity for phosphate sorption when various substances were present in the solution. The dominant role of ligand exchange (replacement of surface  $\text{CO}_3^{2-}$  groups by phosphate) on  $\text{PO}_4\text{-P}$  removal was indicated by the IR-ATR analysis, the pH-independent removal efficiency, the increase of final solution pH and the sequential desorption study. Surface precipitates of Ca-P complexes were confirmed by the SEM-EDS analysis. The major P speciation on the loaded CaT-Z at both low and high initial P concentration was the Ca associated P which is poorly mobilizable in water, suggesting a suitable application of P loaded CaT-Z as slow-release fertilizer in the agriculture. Concluding, CaT-Z presents a promising sorbent for tertiary wastewater treatment, which was chemically modified by an environmental friendly and simple procedure. The relative large particle size of CaT-Z (1.19-2 mm) used in this study can combine an efficient removal of phosphate with an easier separation of the sorbent from the solution in practical

applications. Further studies are required in order to test CaT-Z with real wastewater and in fixed-bed columns as well as the use of the P loaded CaT-Z as soil amendment.

### Acknowledgements

This research did not receive any specific grant from funding agencies in the public, commercial, or not-for-profit sectors.

### References

- [1] M. Zamparas, I. Zacharias, Restoration of eutrophic freshwater by managing internal nutrient loads. A review, *Sci. Total Environ.* 496 (2014) 551-562.
- [2] A. Alshameri, C. Yan, X. Lei, Enhancement of phosphate removal from water by TiO<sub>2</sub>/Yemeni natural zeolite: Preparation, characterization and thermodynamic, *Microporous Mesoporous Mater.* 196 (2014) 145-157.
- [3] C. Han, Z. Wang, W. Yang, Q. Wu, H. Yang, X. Xue, Effects of pH on phosphorus removal capacities of basic oxygen furnace slag, *Ecol. Eng.* 89 (2016) 1-6.
- [4] P. Loganathan, S. Vigneswaran, J. Kandasamy, N.S. Bolan, Removal and recovery of phosphate from water using sorption, *Crit. Rev. Environ. Sci. Technol.* 44 (2014) 847-907.
- [5] D. Bhardwaj, P. Sharma, M. Sharma, R. Tomar, Removal and slow release studies of phosphate on surfactant loaded hydrothermally synthesized silicate nanoparticles, *J. Taiwan Inst. Chem. Eng.* 45 (2014) 2649-2658.
- [6] N.Y. Acelas, B.D. Martin, D. López, B. Jefferson, Selective removal of phosphate from wastewater using hydrated metal oxides dispersed within anionic exchange media, *Chemosphere* 119 (2015) 1353-1360.



- [7] W. Huang, J. Chen, F. He, J. Tang, D. Li, Y. Zhu, Y. Zhang, Effective phosphate adsorption by Zr/Al-pillared montmorillonite: insight into equilibrium, kinetics and thermodynamics, *Appl. Clay Sci.* 104 (2015) 252-260.
- [8] H. Yin, M. Han, W. Tang, Phosphorus sorption and supply from eutrophic lake sediment amended with thermally-treated calcium-rich attapulgite and a safety evaluation, *Chem. Eng. J.* 285 (2016) 671-678.
- [9] H. Yin, M. Kong, Simultaneous removal of ammonium and phosphate from eutrophic waters using natural calcium-rich attapulgite-based versatile adsorbent, *Desalination* 351 (2014) 128-137.
- [10] D. Guaya, M. Hermassi, C. Valderrama, A. Farran, J.L. Cortina, Recovery of ammonium and phosphate from treated urban wastewater by using potassium clinoptilolite impregnated hydrated metal oxides as N-P-K fertilizer, *J. Environ. Chem. Eng.* 4 (2016) 3519-3526.
- [11] M. Zamparas, A. Gianni, P. Stathi, Y. Deligiannakis, I. Zacharias, Removal of phosphate from natural waters using innovative modified bentonites, *Appl. Clay Sci.* 62–63 (2012) 101-106.
- [12] F. Haghseresht, S. Wang, D. Do, A novel lanthanum-modified bentonite, Phoslock, for phosphate removal from wastewaters, *Appl. Clay Sci.* 46 (2009) 369-375.
- [13] C.o.E. Communities, Council Directive 91/271/EEC of 21 May 1991 concerning urban wastewater treatment (amended by the Commission Directive 98/15/EC of 27 February 1998), (1998).

- [14] A. Drizo, C.A. Frost, J. Grace, K.A. Smith, Physico-chemical screening of phosphate-removing substrates for use in constructed wetland systems, *Water Res.* 33 (1999) 3595-3602.
- [15] C. Jiang, L. Jia, Y. He, B. Zhang, G. Kirumba, J. Xie, Adsorptive removal of phosphorus from aqueous solution using sponge iron and zeolite, *J. Colloid Interface Sci.* 402 (2013) 246-252.
- [16] M. Yang, J. Lin, Y. Zhan, Z. Zhu, H. Zhang, Immobilization of phosphorus from water and sediment using zirconium-modified zeolites, *Environ. Sci. Pollut. Res* 22 (2015) 3606-3619.
- [17] S. Massari, M. Ruberti, Rare earth elements as critical raw materials: Focus on international markets and future strategies, *Resources Policy* 38 (2013) 36-43.
- [18] USGS, Mineral commodity summaries, U.S. Department of the Interior, U.S. Geological Survey, (2016) 194-195.
- [19] D. Guaya, C. Valderrama, A. Farran, C. Armijos, J.L. Cortina, Simultaneous phosphate and ammonium removal from aqueous solution by a hydrated aluminum oxide modified natural zeolite, *Chem. Eng. J.* 271 (2015) 204-213.
- [20] H. Yin, M. Kong, C. Fan, Batch investigations on P immobilization from wastewaters and sediment using natural calcium rich sepiolite as a reactive material, *Water Res.* 47 (2013) 4247-4258.
- [21] I. Perassi, L. Borgnino, Adsorption and surface precipitation of phosphate onto CaCO<sub>3</sub>-montmorillonite: effect of pH, ionic strength and competition with humic acid, *Geoderma* 232-234 (2014) 600-608.

- [22] J. Ma, J. Qi, C. Yao, B. Cui, T. Zhang, D. Li, A novel bentonite-based adsorbent for anionic pollutant removal from water, *Chem. Eng. J.* 200–202 (2012) 97-103.
- [23] G. Markou, V.J. Inglezakis, D. Mitrogiannis, I. Efthimiopoulos, M. Psychoyou, P. Koutsovitis, K. Muylaert, I. Baziotis, Sorption mechanism(s) of orthophosphate onto  $\text{Ca}(\text{OH})_2$  pretreated bentonite, *RSC Advances* 6 (2016) 22295-22305.
- [24] L. Hylander, G. Simán, Plant availability of phosphorus sorbed to potential wastewater treatment materials, *Biol. Fertil. Soils* 34 (2001) 42-48.
- [25] L. Lin, C. Wan, D.-J. Lee, Z. Lei, X. Liu, Ammonium assists orthophosphate removal from high-strength wastewaters by natural zeolite, *Sep. Purif. Technol.* 133 (2014) 351-356.
- [26] G. Markou, O. Depraetere, D. Vandamme, K. Muylaert, Cultivation of *Chlorella vulgaris* and *Arthrospira platensis* with recovered phosphorus from wastewater by means of zeolite sorption, *Int. J. Mol. Sci.* 16 (2015) 4250-4264.
- [27] P.J. Bauer, A.A. Szogi, M.B. Vanotti, Agronomic effectiveness of calcium phosphate recovered from liquid swine manure, *Agron. J.* 99 (2007) 1352-1356.
- [28] T.H. Muster, G.B. Douglas, N. Sherman, A. Seeber, N. Wright, Y. Güzükara, Towards effective phosphorus recycling from wastewater: Quantity and quality, *Chemosphere* 91 (2013) 676-684.
- [29] D.G. Randall, M. Krähenbühl, I. Köpping, T.A. Larsen, K.M. Udert, A novel approach for stabilizing fresh urine by calcium hydroxide addition, *Water Res.* 95 (2016) 361-369.
- [30] F. Xie, F. Wu, G. Liu, Y. Mu, C. Feng, H. Wang, J.P. Giesy, Removal of phosphate from eutrophic lakes through adsorption by in situ formation of magnesium hydroxide from diatomite, *Environ. Sci. Technol.* 48 (2013) 582-590.

- [31] APHA, Standard methods for the examination of water and wastewater,, American Public Health Association, American Water Works Association, Water Environment Federation, Washington DC (1999).
- [32] E. Katsou, S. Malamis, M. Tzanoudaki, K.J. Haralambous, M. Loizidou, Regeneration of natural zeolite polluted by lead and zinc in wastewater treatment systems, *J. Hazard. Mater.* 189 (2011) 773-786.
- [33] G. Neeraj, S. Krishnan, P. Senthil Kumar, K.R. Shriaishvarya, V. Vinoth Kumar, Performance study on sequestration of copper ions from contaminated water using newly synthesized high effective chitosan coated magnetic nanoparticles, *J. Mol. Liq.* 214 (2016) 335-346.
- [34] S. Kilic, G. Toprak, E. Ozdemir, Stability of  $\text{CaCO}_3$  in  $\text{Ca}(\text{OH})_2$  solution, *Int. J. Miner. Process.* 147 (2016) 1-9.
- [35] W. An, X. Zhou, X. Liu, P.W. Chai, T. Kuznicki, S.M. Kuznicki, Natural zeolite clinoptilolite-phosphate composite membranes for water desalination by pervaporation, *J. Membr. Sci.* 470 (2014) 431-438.
- [36] A. Casadellà, P. Kuntke, O. Schaetzle, K. Loos, Clinoptilolite-based mixed matrix membranes for the selective recovery of potassium and ammonium, *Water Res.* 90 (2016) 62-70.
- [37] E.L. Uzunova, H. Mikosch, Adsorption of phosphates and phosphoric acid in zeolite clinoptilolite: Electronic structure study, *Microporous Mesoporous Mater.* 232 (2016) 119-125.

- [38] M.D. Ingram, J.E. Davidson, A.M. Coats, E.I. Kamitsos, J.A. Kapoutsis, Origins of anomalous mixed-alkali effects in ion-exchanged glasses, *Glass science and technology* 73 (2000) 89-104.
- [39] L. Wondraczek, G. Gao, D. Möncke, T. Selvam, A. Kuhnt, W. Schwieger, D. Palles, E.I. Kamitsos, Thermal collapse of SAPO-34 molecular sieve towards a perfect glass, *J. Non-Cryst. Solids* 360 (2013) 36-40.
- [40] C.M. Müller, B. Pejčić, L. Esteban, C.D. Piane, M. Raven, B. Mizaikoff, Infrared Attenuated Total Reflectance Spectroscopy: An Innovative Strategy for Analyzing Mineral Components in Energy Relevant Systems, *Scientific Reports* 4 (2014) 6764.
- [41] B. Chen, M.L. Laucks, E.J. Davis, Carbon dioxide uptake by hydrated lime aerosol particles, *Aerosol Sci. Technol.* 38 (2004) 588-597.
- [42] E. Kamitsos, M. Karakassides, A. Patsis, Spectroscopic study of carbonate retention in high-basicity borate glasses, *J. Non-Cryst. Solids* 111 (1989) 252-262.
- [43] R. Chester, H. Elderfield, The application of infra-red absorption spectroscopy to carbonate mineralogy, *Sedimentology* 9 (1967) 5-21.
- [44] D. Palles, I. Konidakis, C. Varsamis, E. Kamitsos, Vibrational spectroscopic and bond valence study of structure and bonding in Al<sub>2</sub>O<sub>3</sub>-containing AgI–AgPO<sub>3</sub> glasses, *RSC Advances* 6 (2016) 16697-16710.
- [45] S. Wang, Y. Peng, Natural zeolites as effective adsorbents in water and wastewater treatment, *Chem. Eng. J.* 156 (2010) 11-24.
- [46] J. Xie, Z. Wang, D. Fang, C. Li, D. Wu, Green synthesis of a novel hybrid sorbent of zeolite/lanthanum hydroxide and its application in the removal and recovery of phosphate from water, *J. Colloid Interface Sci.* 423 (2014) 13-19.

- [47] S. Jiang, X. Wang, S. Yang, H. Shi, Characteristics of simultaneous ammonium and phosphate adsorption from hydrolysis urine onto natural loess, *Environ. Sci. Pollut. Res* 23 (2016) 2628-2639.
- [48] M. Jian, B. Liu, G. Zhang, R. Liu, X. Zhang, Adsorptive removal of arsenic from aqueous solution by zeolitic imidazolate framework-8 (ZIF-8) nanoparticles, *Colloids and Surfaces A: Physicochemical and Engineering Aspects* 465 (2015) 67-76.
- [49] S. Malamis, E. Katsou, A review on zinc and nickel adsorption on natural and modified zeolite, bentonite and vermiculite: Examination of process parameters, kinetics and isotherms, *J. Hazard. Mater.* 252–253 (2013) 428-461.
- [50] J. Matusik, Arsenate, orthophosphate, sulfate, and nitrate sorption equilibria and kinetics for halloysite and kaolinites with an induced positive charge, *Chem. Eng. J.* 246 (2014) 244-253.
- [51] D. Banerjee, U. Sarkar, D. Roy, Multicomponent adsorption of chlorhexidine gluconate in presence of a cationic surfactant: Role of electrostatic interactions and surface complexation, *J. Environ. Chem. Eng.* 1 (2013) 241-251.
- [52] H. Huang, D. Xiao, R. Pang, C. Han, L. Ding, Simultaneous removal of nutrients from simulated swine wastewater by adsorption of modified zeolite combined with struvite crystallization, *Chem. Eng. J.* 256 (2014) 431-438.
- [53] A.T. Mohd Din, M.A. Ahmad, B.H. Hameed, Riboflavin adsorption onto multi-modal mesoporous carbon synthesized from polyethylene glycol 400, *Chem. Eng. J.* 215–216 (2013) 297-305.

- [54] Z. Pei, Z. Kaiqiang, D. Yu, B. Bo, G. Weisheng, S. Yourui, Adsorption of organic dyes by TiO<sub>2</sub>/yeast-carbon composite microspheres and their in situ regeneration evaluation, *Journal of Nanomaterials* 2015 (2015) 13.
- [55] S. Asman, S. Mohamad, N.M. Sarih, Influence of polymer morphology on the adsorption behaviors of molecularly imprinted polymer-methacrylic acid functionalized  $\beta$ -cyclodextrin, *J. Appl. Polym. Sci.* 132 (2015).
- [56] Z. Wang, M. Xing, W. Fang, D. Wu, One-step synthesis of magnetite core/zirconia shell nanocomposite for high efficiency removal of phosphate from water, *Appl. Surf. Sci.* 366 (2016) 67-77.
- [57] S. Baken, S. Nawara, C. Van Moorlegem, E. Smolders, Iron colloids reduce the bioavailability of phosphorus to the green alga *Raphidocelis subcapitata*, *Water Res.* 59 (2014) 198-206.
- [58] O. Callery, R.B. Brennan, M.G. Healy, Use of amendments in a peat soil to reduce phosphorus losses from forestry operations, *Ecol. Eng.* 85 (2015) 193-200.
- [59] X. Zhang, J. Ma, X. Lu, X. Huangfu, J. Zou, High efficient removal of molybdenum from water by Fe<sub>2</sub>(SO<sub>4</sub>)<sub>3</sub>: Effects of pH and affecting factors in the presence of co-existing background constituents, *J. Hazard. Mater.* 300 (2015) 823-829.
- [60] L. Borgnino, C.E. Giacomelli, M.J. Avena, C.P. De Pauli, Phosphate adsorbed on Fe(III) modified montmorillonite: Surface complexation studied by ATR-FTIR spectroscopy, *Colloids and Surfaces A: Physicochemical and Engineering Aspects* 353 (2010) 238-244.
- [61] A. Kaiserli, D. Voutsas, C. Samara, Phosphorus fractionation in lake sediments—Lakes Volvi and Koronia, N. Greece, *Chemosphere* 46 (2002) 1147-1155.

